

Oscillating central motor networks in pathological tremors and voluntary movements: what makes the difference?

Muthuraman Muthuraman, U. Heute, K. Arning, Abdul Rauf Anwar, R. Elble, Günther Deuschl, Jan Raethjen

Angaben zur Veröffentlichung / Publication details:

Muthuraman, Muthuraman, U. Heute, K. Arning, Abdul Rauf Anwar, R. Elble, Günther Deuschl, and Jan Raethjen. 2012. "Oscillating central motor networks in pathological tremors and voluntary movements: what makes the difference?" *NeuroImage* 60 (2): 1331–39. <https://doi.org/10.1016/j.neuroimage.2012.01.088>.

Oscillating central motor networks in pathological tremors and voluntary movements. What makes the difference?

M. Muthuraman ^{a,*}, U. Heute ^b, K. Arning ^a, A.R. Anwar ^{a,b}, R. Elble ^{a,c}, G. Deuschl ^a, J. Raethjen ^a

^a Department of Neurology, Christian-Albrechts-University, Kiel, Germany

^b Institute for Circuit and System Theory, Christian-Albrechts-University, Kiel, Germany

^c Department of Neurology, Southern Illinois U. School of Medicine, Springfield, USA

Introduction

Parkinsonian and essential tremors are proposed to emerge from oscillations in a central subcortical and cortical motor network. The constituents of these networks as revealed by coherent source analysis of tremor-related MEG activity are similar and include motor centers like cerebellum, thalamus, motor and premotor cortices (Schnitzler et al., 2009; Timmermann et al., 2003) all of which take a well known part in physiological motor control. Consequently, voluntary rhythmic movements in healthy subjects mimicking tremor are represented in the same regions (Parker et al., 1992; Pollok et al., 2004). This is plausible and may be the basis for the interference of pathological tremor oscillations with voluntary movements (Raethjen et al., 2005). But the questions remain as to how the obvious difference between voluntarily controlled movements and self sustained pathological tremor oscillations of PD as opposed to ET are reflected in this motor network.

We hypothesized that these differences can be detected by specifically looking at the differences of the central representation for the frequency components of the rhythmic movements and the type of interaction between the different network components. To detect the

central oscillatory motor network we computed coherence and delay between simultaneously recorded 64-channel EEG and forearm EMG and performed coherent source analysis (DICS) (Gross et al., 2001). Following recent hints that the double tremor frequency (the first harmonic) may play a special role in PD (Raethjen et al., 2009; Sapir et al., 2003) we separately analyzed the higher frequency component and the basic tremor frequency to find differences in their central representation and transmission to or from the periphery. In a second step we looked for the direction of interaction between the different components (sources) of the oscillatory network applying renormalized partial directed coherence (RPDC) (Schelter et al., 2009) on the source signals. This combination of approaches reveals different degrees of network pathology in PD and ET, and typical features beyond the mere central representation distinguishing the central network for voluntary and non-voluntary self-sustained movements.

Subjects and methods

Subjects

Six male and 4 female patients with definite Parkinson's disease, as diagnosed by the London brain-bank criteria, participated after giving their informed written consent (Hughes et al., 1992). Age ranged from 38 to 80 yr (mean: 68 ± 12.3) and disease duration ranged from 2 to 25 yr (mean: 8.05 ± 7.05). Eight male and 2 female patients

* Correspondence author at: Department of Neurology, University of Kiel, Schittenhelmstrasse 10, 24105 Kiel, Germany. Fax: +49 431 5978502.

E-mail address: m.muthuraman@neurologie.uni-kiel.de (M. Muthuraman).

fulfilling consensus diagnostic criteria for classical essential tremor (Deuschl et al., 1998) were similarly recruited. Age ranged from 55 to 83 yr (mean: 69.6 ± 7.7) and disease duration ranged from 4 to 60 yr (mean: 29.6 ± 18.7). Patients were seated in a comfortable chair in a slightly reclined position. Both forearms were supported by firm arm rests up to the wrist joints. The hands were held outstretched against gravity, and the patients were asked to keep their eyes open and fixed on a point about 2 m away.

Tremor was recorded by surface EMG from forearm flexors and extensors using silver chloride electrodes. EEG was recorded in parallel with a standard 64 channel recording system (Neuroscan, Herndon, VA, USA), using a linked mastoid reference. Data were stored in a computer and analyzed off-line. Individual recordings were of 1 to 4 min duration. The number of recordings performed in each patient varied between 2 and 8, depending on the patient's tolerance of the experimental procedure. In the case of the PD patients the re-emergent postural tremor was studied. All the patients included in the study did not show any cognitive function decline and continued normally with their medication during the EEG recording.

Eight male and 2 female healthy volunteers also participated. Age ranged from 29 to 52 yr (mean: 34.5 ± 6.9). All were asked to perform rhythmic movements as fast as possible with their hands for 1 to 2 min. The healthy subjects were asked to keep the rhythmic movements in a self-paced manner. The rhythmic movements were checked from each subject by looking at the EMG activity online to have at least 2–5 bursts per second. Four of the subjects could not sustain the movements for 1 min and therefore performed the task twice.

Data pre-processing

EEG and EMG were sampled at 1000 Hz and band-pass filtered (EMG 30–200 Hz; EEG 0.05–200 Hz). EMG was full-wave rectified; the combination of band-pass filtering and rectification is the common demodulation procedure for tremor EMG (Journee, 2007). Each record was segmented into a number of 1 s-long high-quality epochs (L) discarding all those data sections with visible artifacts. The recorded total length of the data for PD (min: 40; max: 185; mean: 150.7 s), ET (min: 65; max: 199; mean: 148.3 s) and HS (min: 65; max: 240; mean: 149.8 s) was not significantly different within subjects between each group. For each record, depending on the length (N) of the recording and the quality of the data, between 40 and 240 1-s segments (M) were used for analysis such that $N = LM$.

Coherence and delay analysis

The coherence spectrum was estimated using the Welch periodogram method with disjoint segments. The statistical significance (Halliday et al., 1995) of the coherence at a particular frequency is calculated by $1 - (1 - \chi)^{1/(M-1)}$, where χ is set to 0.99, so that the confidence limit is $1 - 0.01^{1/(M-1)}$. Values of coherence above this confidence limit are considered to indicate correlation between the two time series, while values below this limit indicate the absence of correlation. The delay was estimated using the maximizing coherence method (Govindan et al., 2005). The significance of the delay τ is checked by the confidence limit, and in order to obtain the variability in the estimated delay, we adapt a so-called surrogate analysis as described in our earlier work (Muthuraman et al., 2008a). This maximizing coherence delay-estimation method (Govindan et al., 2005) was used to estimate the corticomuscular and source signal delays.

Time frequency analysis

The dynamics of signals in the time and frequency domains were computed with the multitaper method (Mitra and Pesaran, 1999). In

this method, the spectrum is estimated by multiplying the data $x(t)$ with ($K=7$) different windows (i.e. tapers). The complete description of the method is explained elsewhere (Muthuraman et al., 2010a). The time step was 50 ms with overlapping windows of 1000 ms, a coherence value is estimated every 50 ms and the frequency resolution is 1 Hz. In a further analysis, all original coherence estimates of the significantly coherent EEG electrodes with the EMG were combined to get a pooled coherence estimate. This can be done by pooling the individual second order spectra using a weighting scheme and estimating the pooled estimate of coherence as previously described (Amjad et al., 1997; Rosenberg et al., 1989). From the pooled time frequency spectrum over the electrodes, the correlation between the basic tremor frequency and the double tremor frequency was estimated for all patients and healthy subjects.

Source analysis

Dynamic imaging of coherent sources (DICS) was used to localize brain activity that is coherent with a peripheral EMG signal (Gross et al., 2001). In order to locate the origin of a specific EEG activity seen on the scalp, two problems need to be solved which are the forward and inverse problems.

The forward problem is the computation of the scalp potentials for a set of neural current sources. It is usually solved by estimating the so-called lead-field matrix with specified models for the brain; a volume conduction model is used with a boundary-element method (BEM) (Fuchs et al., 2002). In our case the brain is modeled by a complex five-concentric-spheres model (De Munck, 2002; van Uitert and Johnson, 2000) with a single sphere for each layer corresponding to the white matter, gray matter, cerebral spinal fluid (CSF), skull and skin.

The inverse problem is finding the relation between the underlying neural activities to the electromagnetic field in the surface. This can be solved by a linear transformation which is done by the spatial filter (van Veen et al., 2002). The spatial filter attenuates the signals from other locations and allows only signals generated from a particular location in the brain for a certain frequency band. The complete description of the forward and the inverse solution is described elsewhere (Muthuraman et al., 2008b, 2010b).

DICS is a beam-forming technique (Gross and Ioannides, 1999; Sekihara and Scholz, 1996) that uses a spatial filter (van Veen et al., 2002) to compute tomographic maps of cerebromuscular coherence at the frequency band of interest. The spatial filter was applied to a large number of voxels covering the entire brain, assigning to each voxel a specific value of coherence to a given reference signal. A voxel size of 5 mm was used in this study. The source in the brain with strongest coherence to the EMG signal at the basic tremor frequency was identified. Since the coherence between the identified areas with it is always 1, this region was projected out of the coherence matrix and further coherent areas were identified (Gross et al., 2002) by taking the EMG as the reference signal. Once coherent brain areas were identified, their activity was extracted by the spatial filter (van Veen et al., 2002). The criteria used to identify areas were done by a within subject surrogate analysis to define the significance level and this was the limit for projecting out and identifying other areas in the brain. The individual maps of strongest cerebromuscular coherence were spatially normalized, averaged and displayed on a standard MNI template brain in SPM2. Local maxima in the resulting maps represent areas that have the strongest coherence to the reference signal. The same procedure was followed separately to find the network of sources for the double tremor frequency. The source analysis was repeated for selective concatenated time intervals for all patients and healthy subjects (mean: 30 ± 1.2)s. The first criterion for selecting the time intervals on the basis of the time frequency analysis was coherence values greater than (mean + std) the whole data length. The second criterion was a coherence difference between the two frequencies greater than the mean value of all the coherence values. If both the conditions

were satisfied these time segments were selected as higher coherence value segments and used for further analysis.

Partial directed coherence

Renormalized partial directed coherence (RPDC) (Schelter et al., 2009) is a technique performed in the frequency domain to detect causal influences in multivariate stochastic systems and provides information on the direction of information flow between the source signals and EMG. The multivariate model was used to model the source signals which use an autoregressive process to obtain the coefficients of the signals in the defined frequency band. In order to obtain these coefficients the correct model order needs to be chosen which was estimated by minimizing the Akaike Information Criterion (AIC) (Akaike, 1974) and gives the optimal order for the corresponding signal (Ding et al., 2000). The AIC was estimated for the whole time series in each subject. The typical range of the model order was between 25 and 30. The frequency band which was investigated in the case of the tremor patients is the individual basic tremor frequencies and the mimicked voluntary rhythmic basic frequencies for the healthy subjects. After estimating the RPDC values the significance level was calculated from the applied data using a bootstrapping method (Kaminski et al., 2001). In the bootstrapping method we divide original time series into smaller non-overlapping windows of equal size. These smaller windows are then shuffled randomly and concatenated. This concatenated time series has the same power spectrum as that of original time series, however all the coherence and directionality are lost. In this paper the open source matlab package ARFIT (Neumaier and Schneider, 2001; Schneider and Neumaier, 2001) was used for estimating the autoregressive coefficients from the spatially filtered source signals.

Statistical analysis

The total data length between the groups was tested with a non-parametric Kruskal-Wallis test for independent samples ($n = 10$, $\alpha = 0.01$). The statistical significance of the corticomuscular delays ($n = 10$, $\alpha = 0.01$; directions are EEG-EMG and EMG-EEG), source signal delays ($n = 10$, $\alpha = 0.01$; directions are TH_PSMC and PSMC_TH) and the time frequency correlation values ($n = 10$, $\alpha = 0.05$; correlation between basic tremor frequency and the double tremor frequency coherence values) was tested using a non-parametric Kruskal-Wallis test followed by post hoc Mann-Whitney testing for independent samples. We carried out three different statistics test on the source level;

1. The significance of the sources was tested by a within subject surrogate analysis. The surrogates were estimated by a Monte Carlo random permutation 100 times shuffling of one second segments within each subject. Estimated the p-value for each of these 100 random permutations.
2. The voxel coordinates with the maximum coherence were compared between PD, ET and HS for all sources present at the basic frequency. The distance (d) was estimated between the voxel coordinates of one source and tested against (d vs. 0). In this case a distance that is not significantly different from 0 indicates that the maximum voxel is in the same location for both groups that are compared (e.g. PD vs. ET or ET vs. HS). The distance was estimated for each combination between the groups in our case 30 subjects (10 in each diagnosis) which resulted in 300 combinations. The chi-square variance test was used to test the distance by defining the category with the minimum as zero and the maximum depending on the calculated distance in each combination. Bonferroni's correction was done, for three comparisons the level of significance would drop from 0.05 to 0.017 between all three combinations (PD vs. ET, ET vs. HS and PD vs. HS).

3. The method used above was also used to compare the sources for the basic frequency and the first harmonic within each group.

The RPDC values ($n = 10$, $\alpha = 0.01$) between the source signals were tested for significance using the multifactorial ANOVA, within-subject factors being the connections of the source signals ($n = 6$: TH_PSMC, PSMC_TH, PSMC_PFC, PFC_PSMC, TH_PFC, PFC_TH), and the between subject factor being the diagnosis ($n = 3$: PD, ET, HS). Finally, the source signal delays were tested for significance using a multifactorial ANOVA, with the within-subject factor being the connections of the source signals ($n = 2$: TH_PSMC, PSMC_TH) and the between subject factor being diagnosis ($n = 3$, PD, ET, HS). The Bonferroni's correction was performed for all the post-hoc tests which involved multiple comparisons.

Results

EEG-EMG coherence

The data length within the subjects between each group was not significantly different ($p = 0.782$). Power spectral analysis on the EMG activity of all three tremors showed a dominant peak at the basic tremor frequency (3–6 Hz) and also at the double tremor frequency (6–12 Hz). At both frequencies, all subjects exhibited significant coherence between EMG and EEG electrodes covering the region of the contralateral sensorimotor cortex.

EEG-EMG delay

The maximizing coherence method (Govindan et al., 2005) was used to analyze the corticomuscular delays at the basic tremor frequency and at the double tremor frequency. All recordings with significant delays showed a bidirectional interaction (EEG-EMG and EMG-EEG). The mean delays in the two directions (positive = EEG-EMG, negative = EMG-EEG) are displayed in (Table 1) for both patient groups and for healthy subjects mimicking tremor. As there were no significant differences between the delays from contralateral cortex to flexor EMG and extensor EMG or between left sided and right-sided muscles in any of the three groups, the two muscle groups of both sides were included in the computed grand mean. The corticomuscular delays for the double tremor frequency were significantly longer than for the basic tremor frequency in PD patients ($p = 0.005$). By contrast, the corticomuscular delays in ET and healthy subjects did not differ significantly ($p = 0.45$) (Table 1).

Dynamics of EEG-EMG coherence over time

Our next step was to analyze the dynamics of these two frequency oscillations over time by applying the multitaper method (Muthuraman et al., 2010a). Fig. 1 shows examples of the time course of the pooled corticomuscular coherence combining the EEG-EMG coherence spectra for all the significantly coherent EEG electrodes (see Subjects and methods). In the right column, the coherence at the double (first harmonic) frequency is plotted versus the coherence at the basic frequency. For Parkinson's patients, the two coherences

Table 1

Corticomuscular and musculocortical delays for the basic tremor frequency and double tremor frequency (first harmonic) for Parkinson's disease (PD) patients, essential tremor (ET) patients and healthy subjects (HS).

Frequency Direction	Basic frequency		First harmonic	
	EEG-EMG	EMG-EEG	EEG-EMG	EMG-EEG
PD	14.18 ± 1.26	-13.70 ± 1.74	19.53 ± 2.18	-18.77 ± 3.01
ET	16.52 ± 2.51	-17.89 ± 2.45	16.24 ± 2.83	-17.46 ± 2.32
HS	16.06 ± 2.46	-18.29 ± 3.16	16.61 ± 3.53	-18.45 ± 2.33

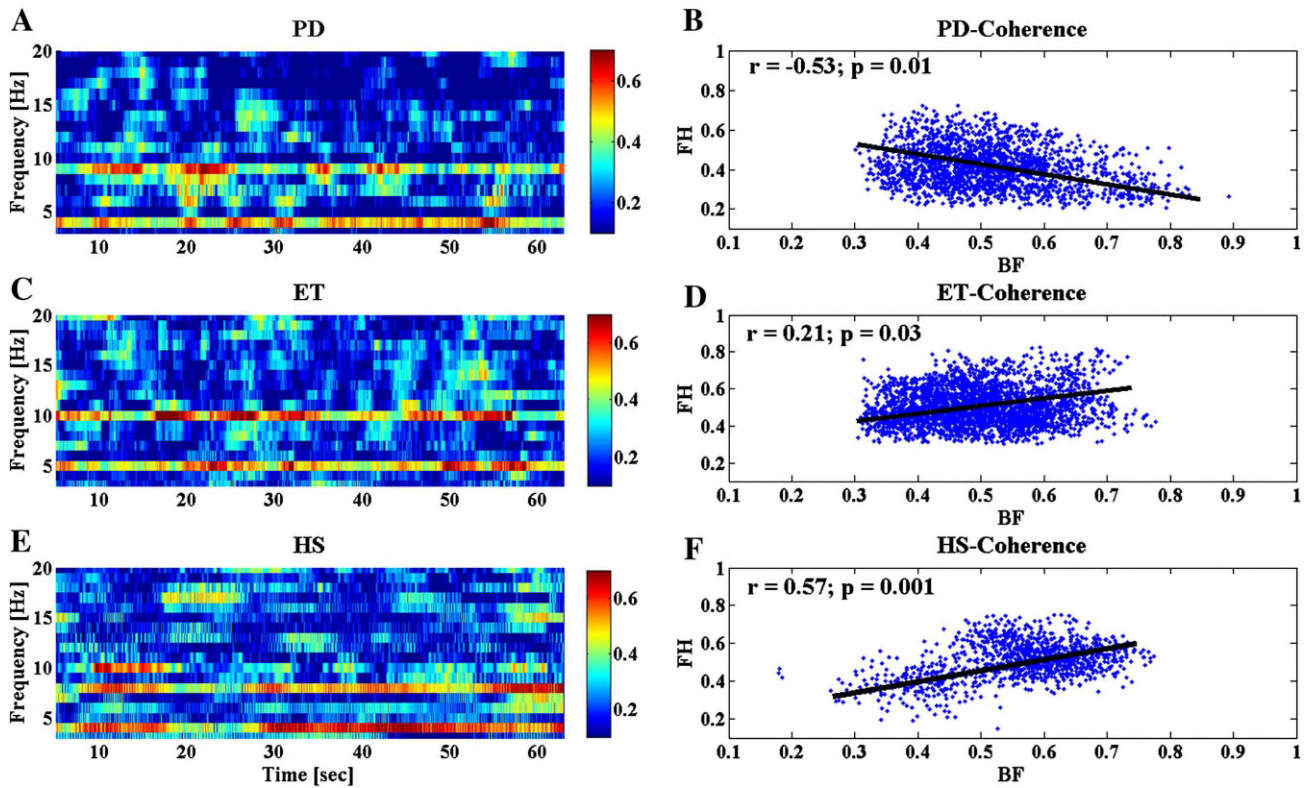


Fig. 1. A. The pooled EEG–EMG coherence over time for a PD patient. B. The correlation of the coherence values between basic tremor frequency (BF) and the double basic tremor frequency (i.e., first harmonic: FH) of the same PD patient. C and D for an ET patient. E and F for a healthy subject.

followed a different time course at the basic tremor frequency and first harmonic, with the cortical correlate of one often being present without the other. Conversely, the time courses in ET and healthy subjects correlated positively (Figs. 1C, D, E & F). The correlation coefficients and significance levels are shown for all subjects and patients in (Table 2). There was a significant correlation between the time course of the two frequency components in all patients and healthy subjects. This correlation was positive in all ET patients and healthy subjects and was negative in all PD patients. However, the positive correlation coefficients were significantly smaller in ET than in healthy subjects ($p = 0.004$), indicating a weaker correlation between the two frequencies in ET (Table 2). These data indicate an alternating central drive at the basic and double tremor frequencies in PD, and a simultaneous drive existed in healthy subjects and ET and was weaker in ET. In order to indicate that it is not a pure peripheral phenomenon the peripheral EMG power was correlated with the dynamics

of the coherence in the patients and healthy subjects and it was not correlated.

Coherent sources

In all PD patients the “double” frequency of the tremor oscillation was not exactly twice the basic tremor frequency (Table 3). Separate runs of the source analysis identified the network responsible for both frequencies. The network for the basic tremor frequency consisted of the PSMC (primary sensory motor cortex), PFC (prefrontal/premotor cortex) and the anterior diencephalon (thalamus) as shown in Fig. 2A. The network for the double tremor frequency was restricted to cortical areas in the region of the PSMC which were adjacent to the PSMC representation of the basic frequency, and there were two additional premotor sources in the vicinity of the PSMC source of the basic frequency and another source in the PPC (posterior

Table 2
Correlation coefficients of the coherence values between the basic tremor frequency and double tremor frequency (first harmonic) for Parkinson’s disease (PD) patients, essential tremor (ET) patients and healthy subjects (HS).

Patient/subject	PD	ET	HS
1	-0.5	0.35	0.49
2	-0.48	0.26	0.56
3	-0.46	0.31	0.43
4	-0.6	0.28	0.62
5	-0.57	0.33	0.67
6	-0.53	0.21	0.53
7	-0.44	0.16	0.6
8	-0.42	0.23	0.47
9	-0.63	0.18	0.64
10	-0.7	0.24	0.7
Mean \pm Std	-0.53 ± 0.09	0.25 ± 0.06	0.57 ± 0.08
p-values	0.001–0.05	0.03–0.05	0.0001–0.001

Table 3
Frequency values of the basic tremor frequency and double tremor frequency (first harmonic) for Parkinson’s disease (PD) patients, essential tremor (ET) patients and healthy subjects (HS) with their mean factors.

Patient/subject	PD		ET		HS	
	Basic	FH	Basic	FH	Basic	FH
1	5	9	6	12	4	8
2	4	9	4	8	5	10
3	3	8	5	10	3	6
4	4	7	6	12	2	4
5	3	7	3	6	5	10
6	6	11	5	10	4	8
7	5	9	4	8	4	8
8	4	9	6	12	5	10
9	4	9	3	6	3	6
10	5	8	5	10	5	10
Mean	4.3	9.1	5.3	10.6	4	8
Factor	2.12		2		2	

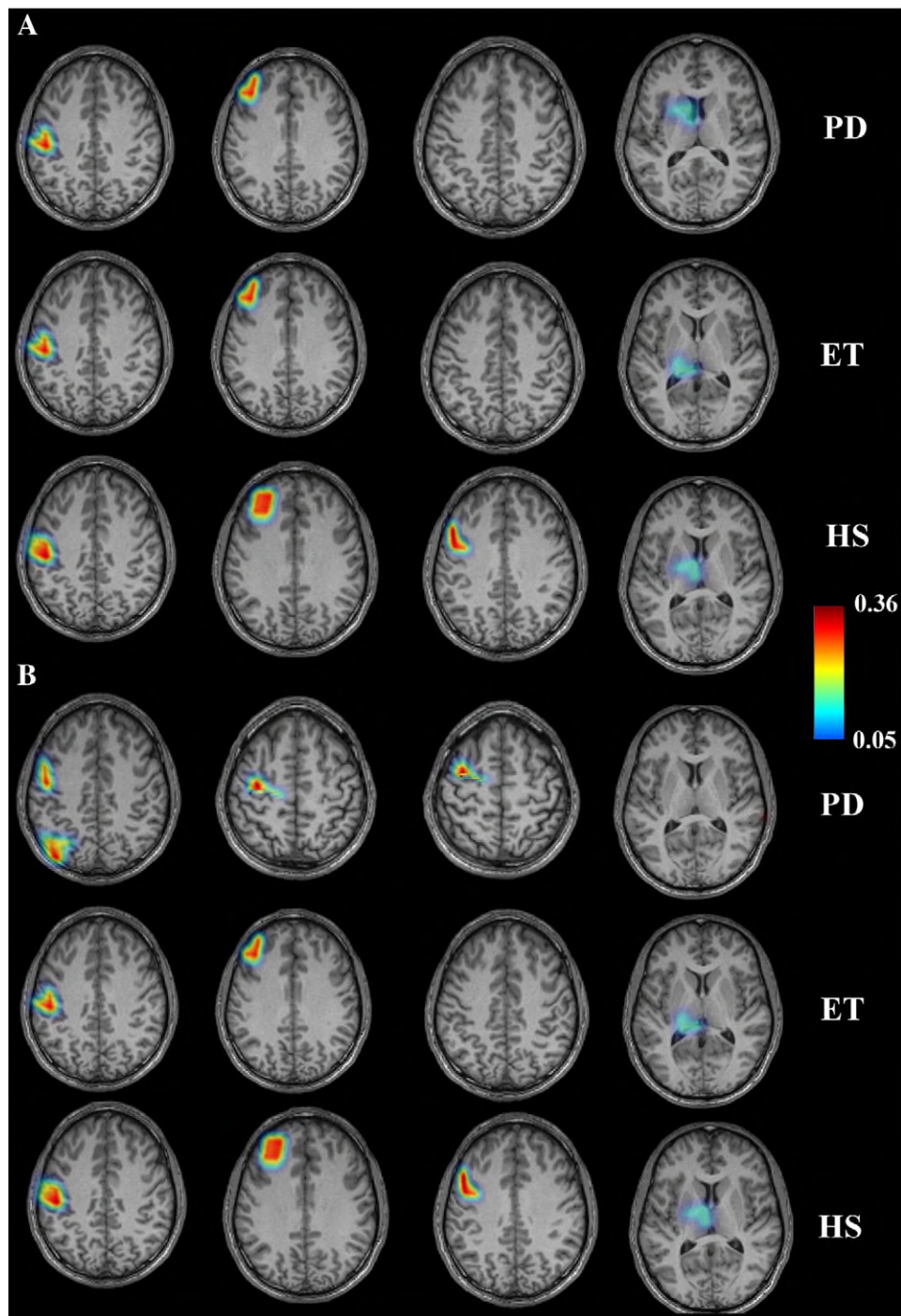


Fig. 2. A. The coherent network of sources for the basic tremor frequency in a Parkinson's disease (PD) patient, in an essential tremor (ET) patient and a healthy subject (HS) and B. the coherent network of sources at the double basic tremor frequency.

parietal cortex). This is illustrated in Fig. 2B group statistic maps of the PD patients.

In all ET patients, the double tremor frequency was exactly twice the basic tremor frequency (Table 3), and the network components were similar for both frequencies. The cortical components in ET were similar to the basic frequency components in PD, but the subcortical source in the diencephalon (thalamus) was more posteriorly located in ET (see Figs. 2A & B group statistic maps from ET patients).

The basic and double-frequency cortical network components of voluntary (mimicked) tremor (Table 3) included PSMC and PFC areas similar to those of the basic- and higher-frequency networks in ET and to those of the basic-frequency network in PD, but the voluntary

networks contained an additional source in another premotor region. Furthermore, the subcortical source at both frequencies for mimicked tremor was in the mid-diencephalon, between the diencephalic sources of PD and ET (Figs. 2A & B). Thus, in contrast to the other two groups, only PD had substantially different cortical networks for the basic and double frequencies, and the diencephalic sources were consistently different for PD, ET and mimicked tremor. For the first two sources 8 out of 10 subjects had the same location and was not statistically different between the groups PD vs. ET ($p = 0.85$); ET vs. HS ($p = 0.87$); PD vs. HS ($p = 0.76$). In case of the third source in the diencephalon the distance was statistically different between the groups (PD vs. ET ($p = 0.009$); ET vs. HS ($p = 0.012$); PD vs. HS ($p = 0.014$)). The sources

for the basic frequency and the first harmonic within each group, showed significant differences for PD ($p = 0.003$) but no significant differences for ET ($p = 0.67$) and HS ($p = 0.78$) for all subjects.

All of these identified sources were statistically significant ($p = 0.004$) in a Monte Carlo random permutation test (see [Subjects and methods](#)) across all subjects within each group. To investigate the interdependence between the separate networks for the two frequencies of Parkinsonian tremor, coherence was computed for all combinations of the spatially filtered source signals of the basic-frequency and double-frequency networks. There was a significant coupling only between the two adjacent PSMC sources of the two frequencies. By looking at concatenated smaller time intervals which satisfies

both the criteria as mentioned ([Source analysis](#)) in which either the basic or the higher frequency was the main EEG–EMG coupling frequency, the main coupling frequency was represented in the whole PD-network comprising all the sources described previously for the basic or double frequency. This is shown in ([Fig. 3A](#)) with group statistic maps and for the basic frequency. It was reproducible during selected time intervals with the above mentioned selection criterion in the [Source analysis](#) in all PD patients and also for the double frequency ([Fig. 3A](#)).

Thus, the two tremor frequency components in PD seem to emerge from different but overlapping networks, which show an intermittent tendency to oscillate. The intermittent access or spill of

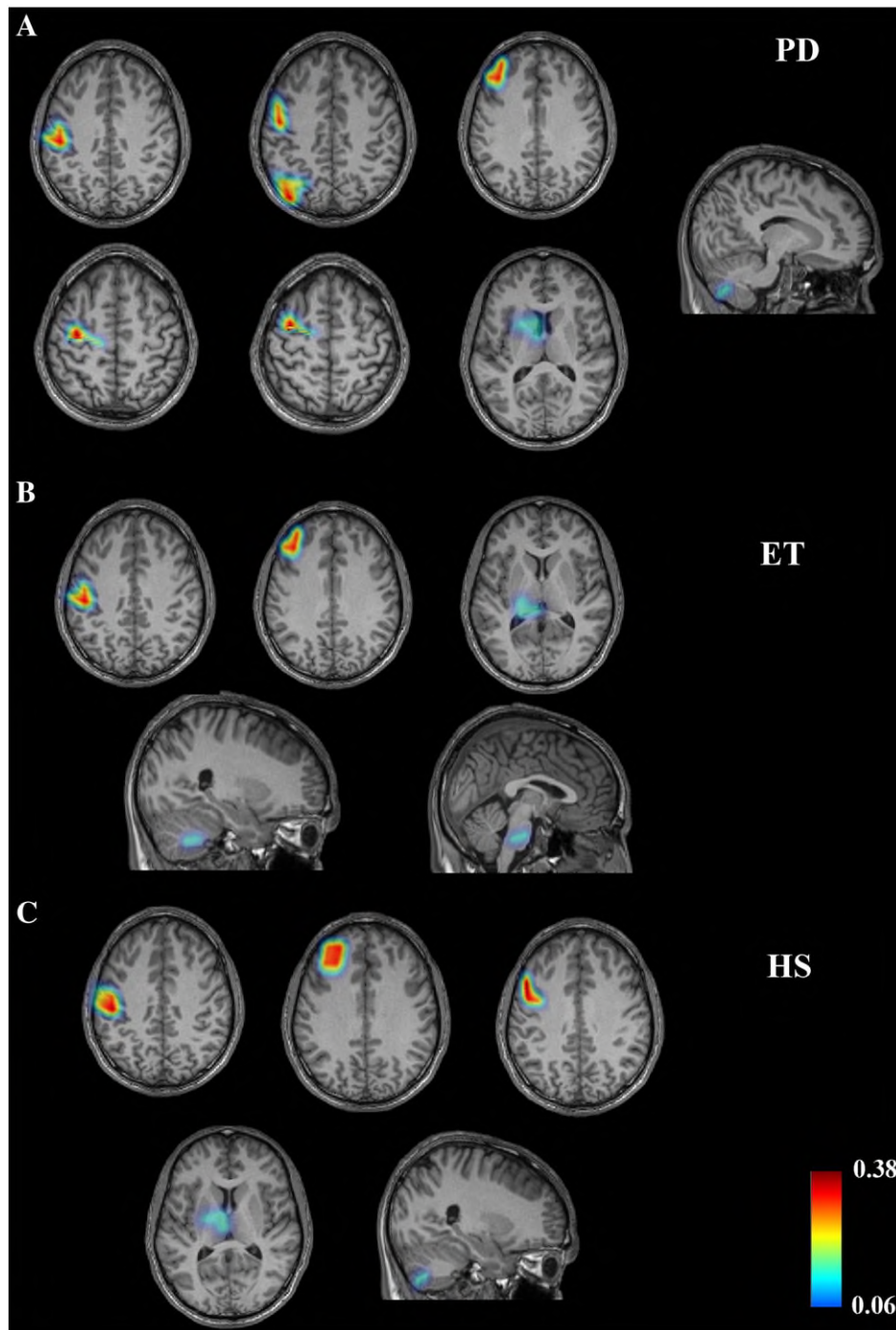


Fig. 3. The coherent network of sources for the basic tremor frequency at selected time intervals with high coherence in a representative Parkinson's disease (PD) patient, B. essential tremor (ET) patient and C. healthy subject (HS).

one of the frequencies into the other frequency's network seems to be via PSMC.

The selective time interval with a higher coherence values as defined in the [Source analysis](#) also revealed one more source in the cerebellum for all PD and ET patients and healthy subjects, as shown in [Fig. 3](#). For ET, another additional source appeared in the brainstem for selected time intervals in all patients ([Fig. 3B](#)). These additional subcortical sources have been described previously in these tremors ([Gross et al., 2001](#); [Schnitzler et al., 2006, 2009](#); [Timmermann et al., 2003](#)) and are probably only detected in phases with higher signal-to-noise ratios in the present study due to the limited electrode array. In our case the electrode array does not have any posterior electrodes below theinion which could be one of the reasons for not detecting the sources in the cerebellum and brainstem.

Delay and directionality between source signals

Renormalized partial directed coherence (RPDC) was estimated between the cortical and sub-cortical source signals ([Fig. 4](#)). The values were statistically compared by ANOVA for repeated measurements and post-hoc comparisons. The RPDC values for diencephalon (thalamus) to PSMC and PFC interaction were significantly higher for healthy subjects ($p=0.006$) compared to the ET and PD patients. The cortical connections from PSMC to PFC and vice versa also were significantly ($p=0.0013$) stronger in healthy subjects. In the within-subject factor analysis, we found a significant difference between interaction from diencephalon to cortical sources (PSMC and PFC) when compared to the opposite direction only in the healthy subjects ($p=0.0062$). These results are illustrated in [Fig. 4](#). The influence of putative additional sources that may not have been identified (e.g. SMA) was tested using two simulations, added as a supplementary material in this paper. The simulations show that the influence is proportional in both directions and does not disturb the general estimation of directionality of information flow by RPDC between those source signals that were detectable (Suppl. Fig. 1).

The transmission delay for the spatially filtered source signals from the diencephalon to the PSMC at the basic tremor frequency was slightly longer for the PD patients compared to the healthy subjects and ET patients. This reached statistical significance ($p=0.002$: between-subject factor of repeated-measures ANOVA and post-hoc comparison, see [Subjects and methods](#)) only for the difference between PD and the voluntarily mimicked tremor ([Fig. 5A](#)). The transmission delay from PSMC to diencephalon was significantly longer ($p=0.005$) for the voluntarily mimicked tremor than for the two pathological tremors ([Fig. 5 B](#)). Most importantly, the difference

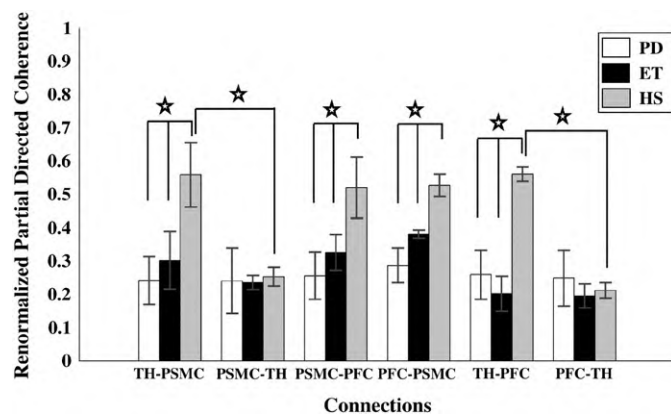


Fig. 4. The mean renormalized partial directed coherence values for the connections thalamus TH-PSMC (primary sensorimotor cortex), TH-PFC (prefrontal cortex), PSMC-TH, PSMC-PFC, PFC-TH and PFC-PSMC at the basic tremor frequency for Parkinson's disease (PD) patients, essential tremor (ET) patients and healthy subjects (HS).

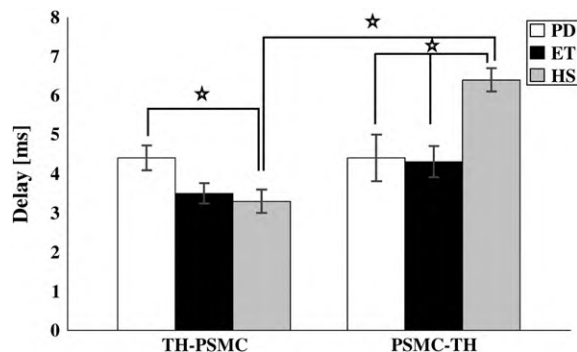


Fig. 5. The mean delay from the thalamus (TH) to the primary sensorimotor cortex (PSMC) and the mean delay from the primary sensorimotor cortex (PSMC) to the thalamus (TH) at the basic tremor frequency for Parkinson's disease (PD) patients, essential tremor (ET) patients and healthy subjects (HS).

between the thalamocortical and corticothalamic delays was significantly different only in the voluntarily mimicked tremor ($p=0.009$: within-subject factor of repeated-measures-ANOVA and post-hoc comparison). Thus, the pathological tremor oscillations in cerebral cortex seemed to be fed back reciprocally to the diencephalon whereas cortical-diencephalic flow took significantly longer and seemed to be less direct than the diencephalic-cortical flow in voluntary tremor.

Discussion

Relation of single and double tremor frequency depends on underlying pathology

Except for the diencephalic source, the cortical representations of the basic tremor frequency in the primary sensorimotor cortex and premotor/prefrontal cortex were the same for both tremors and voluntary movements (mimicked tremor). In fMRI studies, the sequential movements activated similar regions in adults and younger healthy subjects ([Nedelko et al., 2010](#); [Wu and Hallett, 2005](#)). In this review on fMRI studies indicate that more complex tasks induce larger cerebral activation in older than in younger healthy subjects compared to simple motor tasks ([Wars, 2006](#)). In previous studies, additional sources in the region of the SMA and the cerebellum in all tremors and in the brainstem in ET were demonstrated ([Pollok et al., 2004](#); [Schnitzler et al., 2009](#); [Timmermann et al., 2003](#)). The lack of cerebellar and brainstem sources in the present study was probably due to the fact that our sensors did not cover the occipital region, overlying the cerebellum, closer to the brainstem. Nevertheless, in the selective analyses of time segments with strong coherence at the tremor frequency (i.e. increased signal-to-noise-ratio), we were able to identify cerebellar sources in all tremors and a brainstem source in ET, as previously described ([Schnitzler et al., 2009](#)). However, we did not see a coherent source in the region of the SMA. This difference may be due to the use of MEG recordings in previous studies, and MEG may be more sensitive to cortical sources than EEG. Sources in the region of the SMA with a close to perpendicular cortical (dipole) orientation to the skull electrodes may be more readily detected by MEG than EEG ([Ahlfors et al., 2010](#)). In this study the postural tremor has been examined and the identified network may have been modulated by the volitional motoric factors as compared with the "classical" resting tremor.

By performing coherence analyses at both the basic and double tremor frequencies, we are able to differentiate pure first harmonic oscillation from two separate oscillations at these frequencies, as has been recently suggested for Parkinsonian tremor ([Raethjen et al., 2009](#)). In the case of mere harmonics due to waveform asymmetries of the tremor bursts ([Deuschl et al., 1995](#)), we would expect a close correlation with the activity at the basic tremor frequency. We clearly saw

this in the voluntary rhythmic movements. The variations of EEG–EMG coherence at double frequency were positively correlated with those at the basic frequency, and the network components were almost the same. The equality of EEG–EMG delay for both frequencies would be in keeping with a common central origin and pathways of transmission to and from the muscles. A similar situation was found in ET except that the correlation of the basic- and double-frequency coherence at different time segments was significantly weaker than for mimicked tremor. This suggests a tendency of the double tremor frequency to become a separate rhythm, in ET.

A more clearly independent second rhythm at the double basic tremor frequency is seen in PD, and this may be related to the relatively broad range of pathological oscillatory activities in PD, including the 8–12 Hz band of tremor frequency (Salenius et al., 2002). Longer EEG–EMG delays for the double tremor frequency as compared to the basic tremor frequency suggest a different central origin. This is confirmed by the source analysis showing clearly different representations including additional premotor and parietal areas but no subcortical, diencephalic source. The primarily detected cortical source of the higher frequency in PD is directly adjacent albeit distinct from the sensorimotor cortex source of the basic tremor frequency. Coupling between the adjacent cortical sources of the two frequencies was found at the single tremor frequency, in keeping with rhythmic lateral spread or lateral inhibition in the cortex (Llinas et al., 2005).

Different subcortical channels for different tremors

The topography of the diencephalic involvement seems to be different in PD and ET, and both of them in turn differ from the diencephalic source in mimicked tremor. Parkinsonian patients had the most anterior diencephalic sources, whereas the diencephalic source was more posteriorly located in ET, and the source in voluntary tremor was in between these two locations. This is in keeping with deep brain recordings during thalamic surgery in tremor patients in which the cells oscillating at the tremor frequency were on average more posteriorly located in ET than in PD, (Brodkey et al., 2004) and this is also consistent with the known connectivity of the thalamus, with the basal ganglia relay nuclei being more anteriorly located than the cerebellar ones (Jones, 2001). The strikingly systematic difference between the diencephalic sources seems to justify the previous hypothesis that different thalamocortical channels are involved in ET and PD tremors (Deuschl et al., 2000).

There are several reasons why the deep diencephalic sources in our study are probably thalamic. Firstly, these deep sources were consistently located in the vicinity of the thalamus in all patients and normal subjects. Secondly, the thalamus is the bottleneck for all subcortical–cortical interactions. Additional subcortical regions are involved in tremor oscillations (Deuschl et al., 2001) but they must be connected to cerebral cortex via the thalamus no matter from which subcortical regions (e.g. cerebellum, basal ganglia, spinal cord) they may emerge. Thirdly, in a recent study, we were able to validate a coherent thalamic source of epileptic spike activity by event-related fMRI showing activation in almost the same region (Moeller, 2012). Finally, we are not the first to look at tremor related activity by coherent source analysis. Subcortical sources in the region of the thalamus previously have been identified for PD, ET and voluntary tremor (Pollok et al., 2004; Schnitzler et al., 2009; Timmermann et al., 2003). However, previous studies were all MEG-based, which may be slightly inferior to EEG in detecting deep radial sources (Ahlfors et al., 2010), and these studies did not establish the tremor network with respect to the rhythmic EMG signal but to the cortical region with the strongest coherence with EMG (typically M1). Moreover, coherence at the basic and double tremor frequencies was not analyzed separately, as in our study. These differences in methodology may explain the distinguishing features of subcortical sources in our study. However, the probable location error for deep sources due

to the low signal-to-noise-ratio and their projection onto standard brain images preclude a clear allocation of these sources to specific diencephalic structures, and we cannot rule out other structures in this region.

Subcortical–cortical relay in voluntary movements vs. loop oscillations in tremor

In voluntary rhythmic movements, the thalamus has strong bidirectional interactions with connecting cortical sources. The corticothalamic projection was significantly weaker than the thalamocortical projection in our renormalized partial directed coherence analysis, and this result is in keeping with the connectivity pattern described for first-order thalamic relay cells, with a predominance of thalamocortical signaling and modulatory corticothalamic influences (Guillery, 2008). This result is also consistent with the view that voluntary movement emerges from the cerebral cortex, influenced by sensory feedback and modulated by the basal ganglia and cerebellum via the thalamus.

In ET and PD, the interactions were significantly weaker at the cortical level, and the subcortical–cortical interaction did not differ in the two directions, consistent with a reciprocally-connected oscillatory loop. The shorter transmission time (delay) in the loop might reflect a more direct connection between thalamocortical and corticothalamic pathways at the cortical level, participating in tremorogenic oscillation. Modeling studies suggest that such reciprocal and more direct connections favor reverberation and oscillatory entrainment (Crick and Koch, 1998) and such loops have been hypothesized as a basis of normal oscillatory brain activities and other pathological oscillations, such as thalamocortical dysrhythmia (Hughes and Crunelli, 2005; Jones, 2002; Llinas et al., 2005). These brain rhythms are influenced by voluntary behavior but the rhythmic activity itself, like pathological tremor, is not voluntary.

Thus, we suggest on the basis of our data and in line with existing hypotheses that direct and reciprocal corticothalamocortical interactions play an important role in the generation and amplification of oscillations at the tremor frequency (Elble, 2000; Fasano et al., 2010) and these oscillations gain access to the peripheral motor system via corticospinal projections. Conversely, the stronger thalamocortical connectivity in voluntary rhythmic movement is consistent with a voluntary rhythmic activation of relevant cortical neurons and with corticothalamic feedback facilitating the desired thalamocortical activation. The relatively weak and bidirectionally coupled oscillating thalamocortical loop in pathological tremors is conceivably more amenable to therapeutic modulation or disruption with thalamic deep brain stimulation than are the stronger, asymmetric interactions in voluntary movements, thus explaining the selective effect of thalamic deep brain stimulation on tremor, with impairment of voluntary motor control only at suprathreshold stimulation intensities (Fasano et al., 2010; Hauser et al., 1998).

Two distinguishing features of tremor network architecture seem to differentiate the pathologic tremors in ET and PD from voluntary mimicked tremor in normal human subjects. One is the more symmetric and direct (albeit weaker) connections between diencephalic (i.e. thalamic) regions and motor cortex, forming thalamocortical loops that produce or facilitate pathologic tremorogenic oscillation. The other is the tendency of basic- and double-frequency tremor oscillations to occur independently in ET and PD, reflecting the more autonomous nature of pathologic oscillation in both diseases and the more effective changes in tremor network components of PD. Our findings begin to explain the paradox that pathological tremors and voluntary mimicked tremor emerge from similar neuronal pathways, but pathologic tremors cannot be voluntarily controlled. Additional studies are needed to further elucidate the pathophysiologic and microstructural bases of our observations.

Acknowledgments

This work was supported by the German Research Council (SFB 855-Project D2). The funder does not have any involvement in the study design; in the collection, analysis and interpretation of data; in the writing of the report; and in the decision to submit the article for publication.

References

- Ahlfors, S.P., Han, J., Belliveau, J.W., Hamalainen, M.S., 2010. Sensitivity of MEG and EEG to source orientation. *Brain Topogr.* 23, 227–232.
- Akaike, H., 1974. A new look at the statistical model identification. *IEEE Trans. Autom. Control* 19, 716–723.
- Amjad, A.M., Halliday, D.M., Rosenberg, J.R., Conway, B.A., 1997. An extended difference of coherence test for comparing and combining several independent coherence estimates: theory and application to the study of motor units and physiological tremor. *J. Neurosci. Methods* 73, 69–79.
- Neumaier, A., Schneider, T., 2001. Estimation of parameters and eigenmodes of multivariate autoregressive models. *ACM* 27–57.
- Brodkey, J.A., Tasker, R.R., Hamani, C., McAndrews, M.P., Dostrovsky, J.O., Lozano, A.M., 2004. Tremor cells in the human thalamus: differences among neurological disorders. *J. Neurosurg.* 101, 43–47.
- Crick, F., Koch, C., 1998. Constraints on cortical and thalamic projections: the no-strong-loops hypothesis. *Nature* 391, 245–250.
- De Munck, J.C., 2002. A linear discretization of the volume conductor boundary integral equation using analytically integrated elements (electrophysiology application). *IEEE Trans. Biomed. Eng.* 39, 986–990.
- Deuschl, G., Lauk, M., Timmer, J., 1995. Tremor classification and tremor time series analysis. *Chaos* 5, 48–51.
- Deuschl, G., Bain, P., Brin, M., 1998. Consensus statement of the Movement Disorder Society on Tremor. *Ad Hoc Scientific Committee. Mov. Disord.* 13 (Suppl. 3), 2–23.
- Deuschl, G., Raethjen, J., Baron, R., Lindemann, M., Wilms, H., Krack, P., 2000. The pathophysiology of parkinsonian tremor: a review. *J. Neurol.* 247 (Suppl. 5), V33–V48.
- Deuschl, G., Raethjen, J., Lindemann, M., Krack, P., 2001. The pathophysiology of tremor. *Muscle Nerve* 24, 716–735.
- Ding, M., Bressler, S.L., Yang, W., Liang, H., 2000. Short-window spectral analysis of cortical event-related potentials by adaptive multivariate autoregressive modeling: data preprocessing, model validation, and variability assessment. *Biol. Cybern.* 83, 35–45.
- Elble, R.J., 2000. Origins of tremor. *Lancet* 355, 1113–1114.
- Fasano, A., Herzog, J., Raethjen, J., Rose, F.E., Muthuraman, M., Volkmann, J., Falk, D., Elble, R., Deuschl, G., 2010. Gait ataxia in essential tremor is differentially modulated by thalamic stimulation. *Brain* 133, 3635–3648.
- Fuchs, M., Kastner, J., Wagner, M., Hawes, S., Ebersole, J.S., 2002. A standardized boundary element method volume conductor model. *Clin. Neurophysiol.* 113, 702–712.
- Govindan, R.B., Raethjen, J., Kopper, F., Claussen, J.C., Deuschl, G., 2005. Estimation of time delay by coherence analysis. *Physica A* 350, 277–295.
- Gross, J., Ioannides, A.A., 1999. Linear transformations of data space in MEG. *Phys. Med. Biol.* 44, 2081–2097.
- Gross, J., Kujala, J., Hamalainen, M., Timmermann, L., Schnitzler, A., Salmelin, R., 2001. Dynamic imaging of coherent sources: studying neural interactions in the human brain. *Proc. Natl. Acad. Sci. U. S. A.* 98, 694–699.
- Gross, J., Timmermann, L., Kujala, J., Dirks, M., Schmitz, F., Salmelin, R., Schnitzler, A., 2002. The neural basis of intermittent motor control in humans. *Proc. Natl. Acad. Sci. U. S. A.* 99, 2299–2302.
- Guillery, R., 2008. The contributions of anatomical studies to knowledge of perceptual processing. *Anatomy* 2, 9–15.
- Halliday, D.M., Rosenberg, J.R., Amjad, A.M., Breeze, P., Conway, B.A., Farmer, S.F., 1995. A framework for the analysis of mixed time series/point process data—theory and application to the study of physiological tremor, single motor unit discharges and electromyograms. *Prog. Biophys. Mol. Biol.* 64, 237–278.
- Hauser, R.A., Friedlander, J., Smith, D.A., Nolan, M.F., 1998. Delayed stimulation-induced thalamic ataxia syndrome. *Neurology* 50, 1184–1185.
- Hughes, S.W., Crunelli, V., 2005. Thalamic mechanisms of EEG alpha rhythms and their pathological implications. *Neuroscientist* 11, 357–372.
- Hughes, A.J., Daniel, S.E., Kilford, L., Lees, A.J., 1992. Accuracy of clinical diagnosis of idiopathic Parkinson's disease: a clinico-pathological study of 100 cases. *J. Neurol. Neurosurg. Psychiatry* 55, 181–184.
- Jones, E.G., 2001. The thalamic matrix and thalamocortical synchrony. *Trends Neurosci.* 24, 595–601.
- Jones, E.G., 2002. Thalamic circuitry and thalamocortical synchrony. *Philos. Trans. R. Soc. Lond. B, Biol. Sci.* 357, 1659–1673.
- Journee, H.L., 2007. Demodulation of amplitude modulated noise: a mathematical evaluation of a demodulator for pathological tremor EMG's. *IEEE Trans. Biomed. Eng.* 304–308.
- Kaminski, M., Ding, M., Truccolo, W.A., Bressler, S.L., 2001. Evaluating causal relations in neural systems: Granger causality, directed transfer function and statistical assessment of significance. *Biol. Cybern.* 85, 145–157.
- Llinas, R., Urbano, F.J., Leznik, E., Ramirez, R.R., van Marle, H.J., 2005. Rhythmic and dysrhythmic thalamocortical dynamics: GABA systems and the edge effect. *Trends Neurosci.* 28, 325–333.
- Mitra, P.P., Pesaran, B., 1999. Analysis of dynamic brain imaging data. *Biophys. J.* 76, 691–708.
- Moeller, F., Muthuraman, M., Stephani, U., Deuschl, G., Raethjen, J., Siniatchkin, M. in press. Representation and propagation of epileptic activity in absences and generalized photoparoxysmal responses. *Human Brain Mapping* doi:10.1002/hbm22026.
- Muthuraman, M., Govindan, R.B., Deuschl, G., Heute, U., Raethjen, J., 2008a. Differentiating phase shift and delay in narrow band coherent signals. *Clin. Neurophysiol.* 119, 1062–1070.
- Muthuraman, M., Raethjen, J., Hellriegel, H., Deuschl, G., Heute, U., 2008b. Imaging coherent sources of tremor related EEG activity in patients with Parkinson's disease. *Conf. Proc. IEEE Eng. Med. Biol. Soc.* 2008, 4716–4719.
- Muthuraman, M., Galka, A., Deuschl, G., Heute, U., Raethjen, J., 2010a. Dynamical correlation of non-stationary signals in time domain—a comparative study. *Biomed. Signal Process. Control* 5, 205–213.
- Muthuraman, M., Heute, U., Deuschl, G., Raethjen, J., 2010b. The central oscillatory network of essential tremor. *Conf. Proc. IEEE Eng. Med. Biol. Soc.* 1, 154–157.
- Nedelko, V., Hassa, T., Hamzei, F., Weiller, C., Binkofski, F., Schoenfeld, M.A., Tüscher, O., Dettmers, C., 2010. Age-independent activation in areas of the mirror neuron system during action observation and action imagery. A fMRI study. *Restor. Neurol. Neurosci.* 737–747.
- Wars, N.S., 2006. Compensatory mechanisms in the aging motor system. *Ageing Res. Rev.* 5, 239–254.
- Parker, F., Tzourio, N., Blond, S., Petit, H., Mazoyer, B., 1992. Evidence for a common network of brain structures involved in Parkinsonian tremor and voluntary repetitive movement. *Brain Res.* 584, 11–17.
- Pollok, B., Gross, J., Dirks, M., Timmermann, L., Schnitzler, A., 2004. The cerebral oscillatory network of voluntary tremor. *J. Physiol.* 554, 871–878.
- Raethjen, J., Pohle, S., Govindan, R.B., Morsnowski, A., Wenzelburger, R., Deuschl, G., 2005. Parkinsonian action tremor: interference with object manipulation and lacking levodopa response. *Exp. Neurol.* 194, 151–160.
- Raethjen, J., Govindan, R.B., Muthuraman, M., Kopper, F., Volkmann, J., Deuschl, G., 2009. Cortical correlates of the basic and first harmonic frequency of Parkinsonian tremor. *Clin. Neurophysiol.* 120, 1866–1872.
- Rosenberg, J.R., Amjad, A.M., Breeze, P., Brillinger, D.R., Halliday, D.M., 1989. The Fourier approach to the identification of functional coupling between neuronal spike trains. *Prog. Biophys. Mol. Biol.* 53, 1.
- Salenius, S., Avikainen, S., Kaakkola, S., Hari, R., Brown, P., 2002. Defective cortical drive to muscle in Parkinson's disease and its improvement with levodopa. *Brain* 125, 491–500.
- Sapir, N., Karasik, R., Havlin, S., Simon, E., Hausdorff, J.M., 2003. Detecting scaling in the period dynamics of multimodal signals: application to Parkinsonian tremor. *Phys. Rev. E, Stat. Nonlin. Soft Matter Phys.* 67, 031903.
- Schelter, B., Timmer, J., Eichler, M., 2009. Assessing the strength of directed influences among neural signals using renormalized partial directed coherence. *J. Neurosci. Methods* 179, 121–130.
- Schnitzler, A., Timmermann, L., Gross, J., 2006. Physiological and pathological oscillatory networks in the human motor system. *J. Physiol. Paris* 99, 3–7.
- Schnitzler, A., Munks, C., Butz, M., Timmermann, L., Gross, J., 2009. Synchronized brain network associated with essential tremor as revealed by magnetoencephalography. *Mov. Disord.* 24, 1629–1635.
- Sekihara, K., Scholz, B., 1996. Generalized Wiener estimation of three-dimensional current distribution via biomagnetic measurements. *IEEE Trans. Biomed. Eng.* 43, 281–291.
- Schneider, T., Neumaier, A., 2001. Algorithm 808: ARfit—a matlab package for the estimation of parameters and eigenmodes of multivariate autoregressive models. *ACM* 58–65.
- Timmermann, L., Gross, J., Dirks, M., Volkmann, J., Freund, H.J., Schnitzler, A., 2003. The cerebral oscillatory network of parkinsonian resting tremor. *Brain* 126, 199–212.
- van Uiter, R., Johnson, C., 2000. Can a spherical model substitute for a realistic model in forward and inverse MEG simulations. *Biomagnetism J.* 1, 1–3.
- van Veen, B.D., van Drongelen, W., Yuchtman, M., Suzuki, A., 2002. Localization of brain electrical activity via linearly constrained minimum variance spatial filtering. *IEEE Trans. Biomed. Eng.* 44, 867–880.
- Wu, T., Hallett, M., 2005. The influence of normal human ageing on automatic movements. *J. Physiol.* 562, 605–615.